Supporting Information

8x2 transceiver

Demonstration of the 8x2 transceiver at 7T has been previously presented at the 10th biennial High and ultra-high field MR imaging Workshop, October 1-3 2015 Minneapolis MN USA. In this work, we used 8 independent transmit channels driven in two configurations. Configuration A uses a single RF channel to drive two adjacent coils within a row to maximize phase and amplitude adjustment between rows which thus makes use of the smaller size and higher efficiency of the superior row. Configuration B uses a single RF channel to drive two longitudinally adjacent coils to maximize phase and amplitude adjustment within a row, thereby maximizing in-plane phase flexibility (Figure S1).

Figure S1: Two configurations are shown for driving the 8x2 transceiver from 8 independent RF channels. Configuration A: a single RF channel drives two adjacent coils within a row. Configuration B: a single RF channel drives two longitudinally adjacent coils.

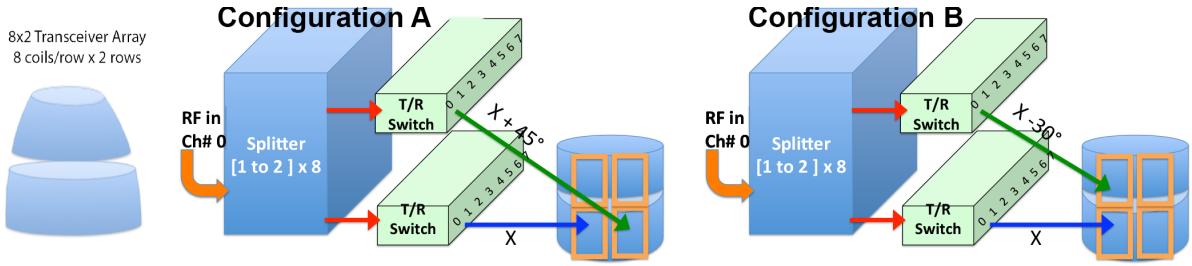

Displayed in Fig. S2A,B are orthogonal slices from a 3D MP2RAGE image demonstrating the extent of coverage for the 8x2 array in both configurations. For both configurations, a B_1 amplitude of 17.6μT (750Hz) was reached for all subjects with all RF drive voltages below 150V and most below 120V. Fig. S2D,E display B_1 maps for the homogeneous distribution for both configurations using a single set of amplitudes and phases for all slices. Although configuration A achieves superior homogeneity over the entire brain within the slice (Fig S2C - SD=10.4±1.8%, n=8 subjects) configuration B also achieves good homogeneity (SD=11.8±3.1%, n=10 subjects). For configuration B, the use of a single drive voltage for coils in different rows results in gradient of increasing RF amplitude along the Z-axis. Displayed in Fig S2F are B_1 maps for configuration B showing the ring distribution. Pertinent for MR spectroscopic imaging applications, the ring distribution allows a purely B1+ based avenue for spatial localization, e.g., for superficial skull and skin lipid outer volume suppression.

Figure S2: Experimental data showing performance of the two configurations. For each configuration, the MP2RAGE and B1 maps are shown. With configuration B, two RF distributions can be defined to excite the "homogeneous" volume and a "ring" volume.

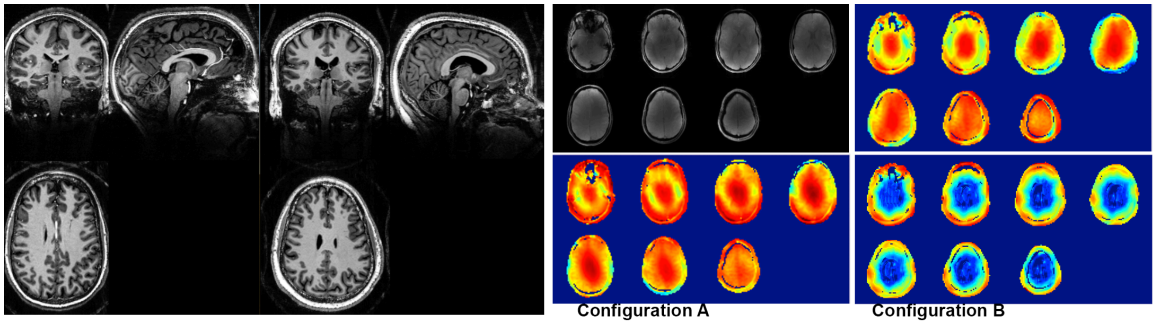

Alternate timing of T2 spin echo preparation weighting

The application of the spin echo weighting can be applied either early or late in the inversion recovery. While this paper reports on the strategy and implemented methods based on an early spin echo, the spin echo can also be applied after the null in the inversion recovery to generate a CSF suppressed T2 weighted image. For a two-block sequence, the results are similar to that seen with the early spin echo acquisition, although there are

some differences due to the different speed of T1 recovery between tissue types during the latter portion of the inversion timecourse. For example, Figure S3 shows such a case of ti1/ti2/TR/TE 1.7/2.5/5/125ms, which shows CSF suppression and a sharp incline in calculated signal over increasing T2.

Figure S3: Bloch simulations of a late T2 preparation two block acquisition, S_1 and S_2. (A) The timecourse of Iz amplitudes is shown (5 tissue components: CSF blue, GM black, WM red with inversion, pathologic T2. Note that the time axis is not linear, with each unit representing a simulation step. (B) The surface plots of the signal amplitudes are shown over the [T1, T2] parameter space for S_1, S_2 and the calculated signal $R_{1/2}$ (using Eq. 1 from text). The calculated $R_{1/2}$ shows the CSF suppression and signal enhancement over the pathologic range of T2. The black dots on the surface plots indicate the 5 tissue components. T1, T2 values for CSF are assigned at 4.3s, 0.9s; GM 2.0s, 60ms; WM 1.2s, 60ms.